RESEARCH ARTICLE

Figures and figure supplements

Fitness landscape of substrate-adaptive mutations in evolved amino acid-polyamine-organocation transporters

Foteini Karapanagioti *et al*.

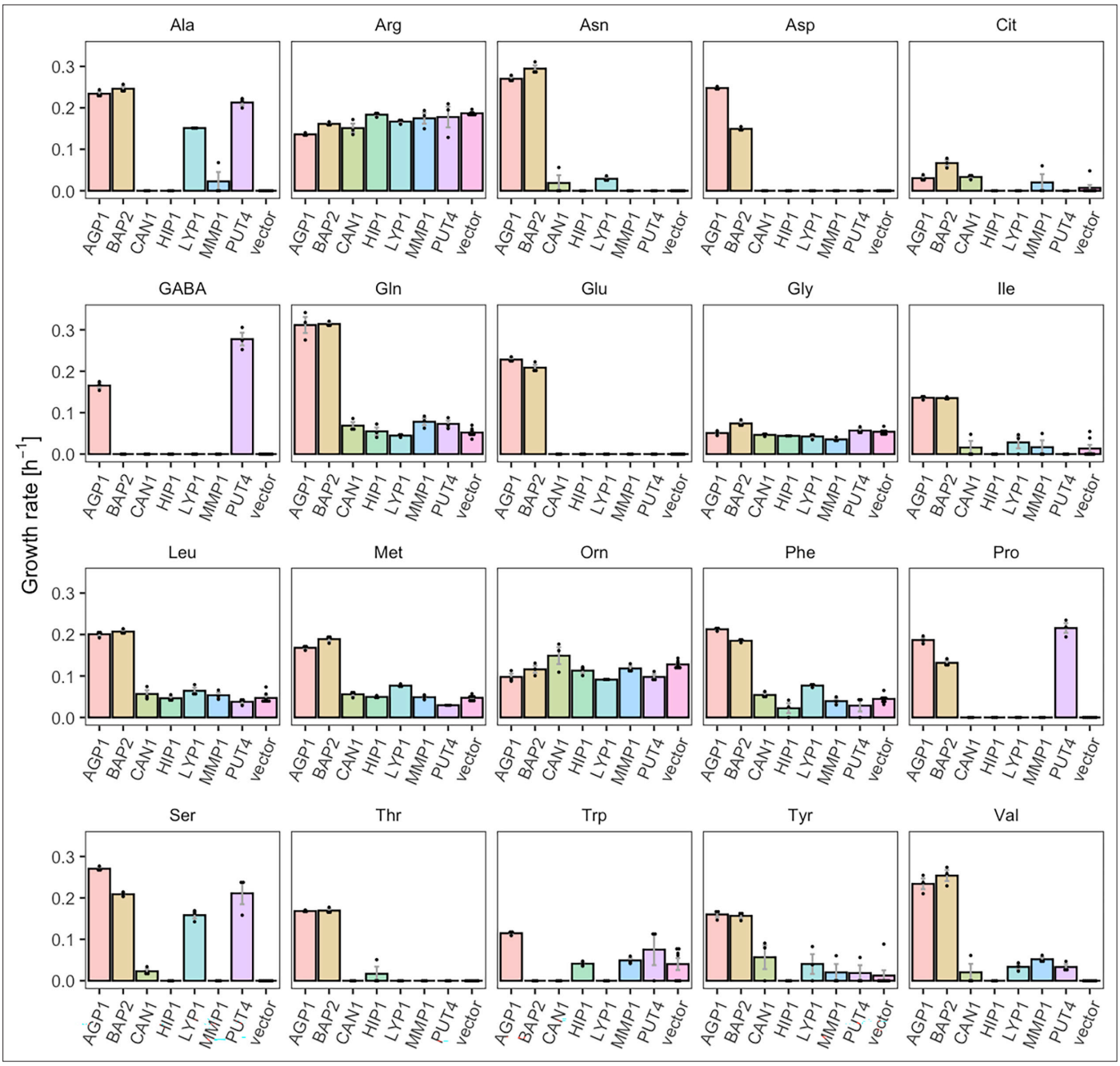

Figure 1. Yeast amino acid transporters (YAT) support growth on a range of amino acids. Growth rates of Δ10AA expressing one of seven different wild-type YAT genes (*AGP1*, *BAP2*, *CAN1*, *HIP1*, *LYP1*, *MMP1*, *PUT4*) from pADHXC3GH and the empty vector control on 2 mM of each amino acid. Error bars represent the SEM (n≥3). For the respective growth curves, see ***Figure 1—figure supplement 1***. For the respective growth rates, see ***Figure 1—source data 1***. To give an indication of the relatedness of YAT proteins from *S. cerevisiae*, a pairwise identity matrix based on Clustal Omega (***Madeira et al., 2022***) alignment of Uniprot (***UniProt Consortium, 2023***) sequences is presented in ***Figure 1—figure supplement 2***.

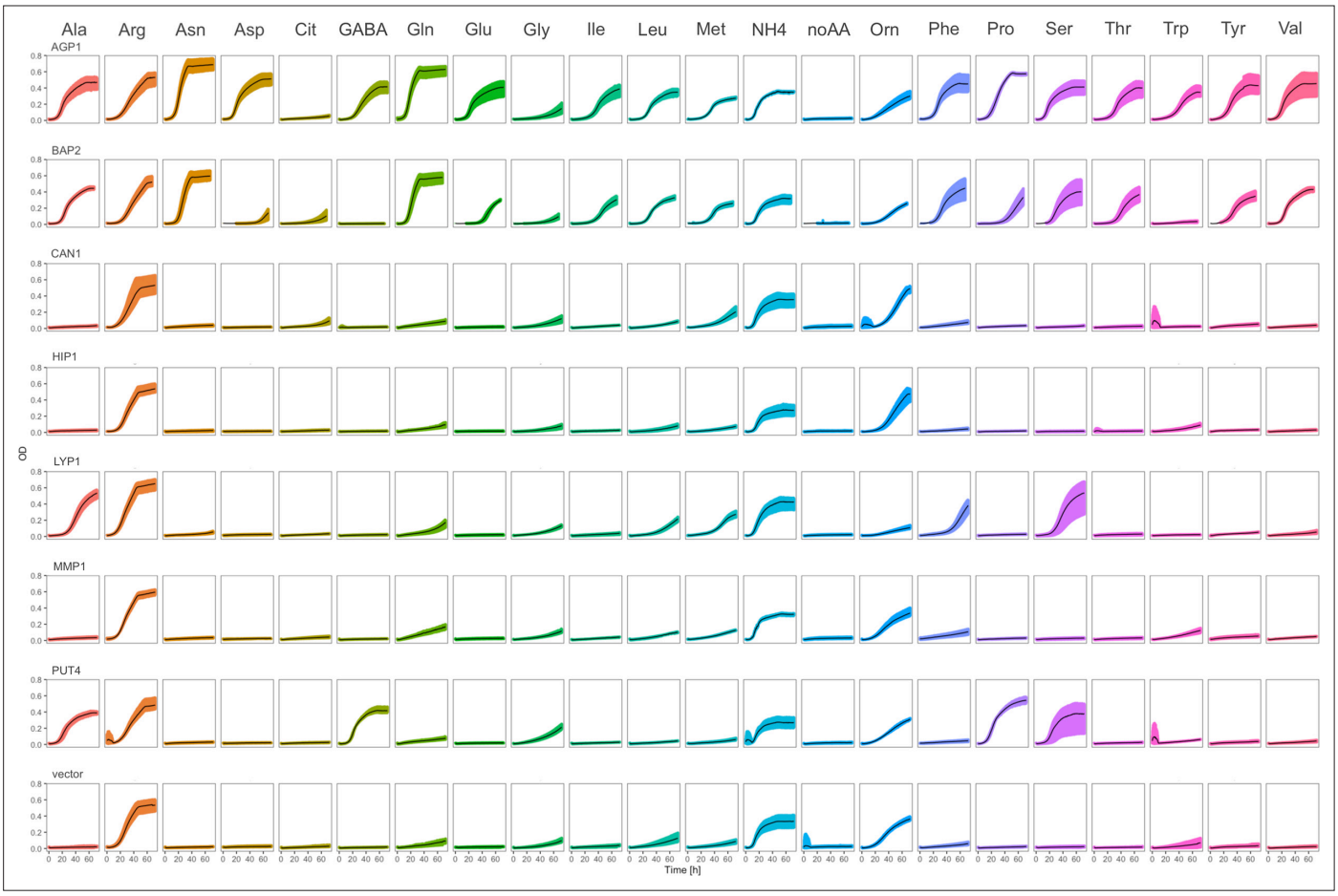

Figure 1—figure supplement 1. Yeast amino acid transporters (YAT) support growth on a range of amino acids. Growth curves of Δ10AA expressing either one of the seven different wild-type YAT genes (*AGP1*, *BAP2*, *CAN1*, *HIP1*, *LYP1*, *MMP1*, *PUT4*) from pADHXC3GH and the empty vector control on 2 mM of each amino acid. Black lines represent mean values of all measured curves (n≥3). Colored areas represent the SD range.

	TAT1	BAP2	BAP3	AGP1	GNP1	MMP1	SAM3	TAT2	GAP1	HIP1	AGP2	AGP3	PUT4	DIP5	LYP1	ALP1	CAN1
TAT1	100	51	49	53	53	36	35	39	43	38	22	27	30	29	31	31	31
BAP2	51	100	73	53	54	37	38	40	44	43	24	29	31	30	34	33	33
BAP3	49	73	100	51	53	36	35	39	41	41	22	27	27	29	31	32	30
AGP1	53	53	51	100	68	39	39	40	44	40	25	27	29	30	32	33	32
GNP1	53	54	53	68	100	36	36	41	44	39	23	26	27	29	31	32	32
MMP1	36	37	36	39	36	100	70	38	44	41	24	28	28	31	33	32	32
SAM3	35	38	35	39	36	70	100	39	47	44	23	27	28	31	32	32	33
TAT2	39	40	39	40	41	38	39	100	46	43	25	27	30	32	33	35	32
GAP1	43	44	41	44	44	44	47	46	100	51	28	32	31	32	37	36	36
HIP1	38	43	41	40	39	41	44	43	51	100	26	29	32	32	33	32	34
AGP2	22	24	22	25	23	24	23	25	28	26	100	24	31	28	29	28	26
AGP3	27	29	27	27	26	28	27	27	32	29	24	100	28	31	31	33	33
PUT4	30	31	27	29	27	28	28	30	31	32	31	28	100	37	34	34	35
DIP5	29	30	29	30	29	31	31	32	32	32	28	31	37	100	36	36	37
LYP1	31	34	31	32	31	33	32	33	37	33	29	31	34	36	100	59	62
ALP1	31	33	32	33	32	32	32	35	36	32	28	33	34	36	59	100	67
CAN1	31	33	30	32	32	32	33	32	36	34	26	33	35	37	62	67	100

Figure 1—figure supplement 2. Pairwise identities of yeast amino acid transporter (YAT) protein sequences from *S. cerevisiae*. The multiple sequence alignment was performed using Clustal Omega, with standard UniProt protein sequences as input (*AGP1*: P25376, *AGP2*: P38090, *AGP3*: P43548, *ALP1*: P38971, *BAP2*: P38084, *BAP3*: P41815, *CAN1*: P04817, *DIP5*: P53388, *GAP1*: P19145, *GNP1*: P48813, *HIP1*: P06775, *LYP1*: P32487, *MMP1*: Q12372, *PUT4*: P15380, *SAM3*: Q08986, *TAT1*: P38085, *TAT2*: P38967). The sequence identity is shown in percentage, from no identity (0) to identical match (100), represented in blue and red respectively.

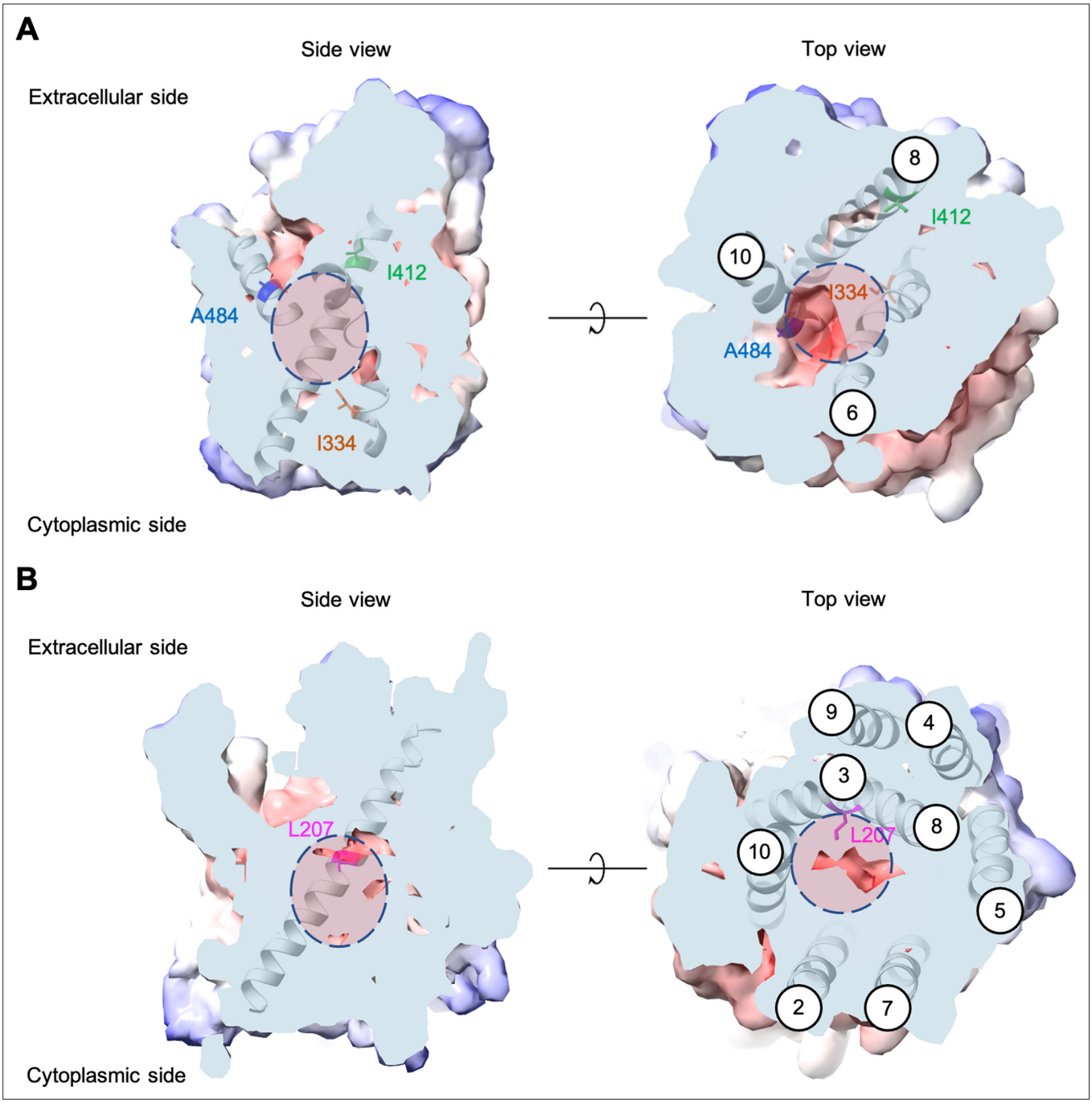

Figure 2. Positions of the substituted amino acids investigated in this study. Side and top views of the AlphaFold models of *AGP1* (AF-P25376) (**A**) and *PUT4* (AF-P15380) (**B**) visualized in ChimeraX (1.3.0) (***Pettersen et al., 2021***). The amino acids of interest are highlighted in different colors. The respective TMs are presented in circles. The predicted substrate binding site is represented as dashed circle.

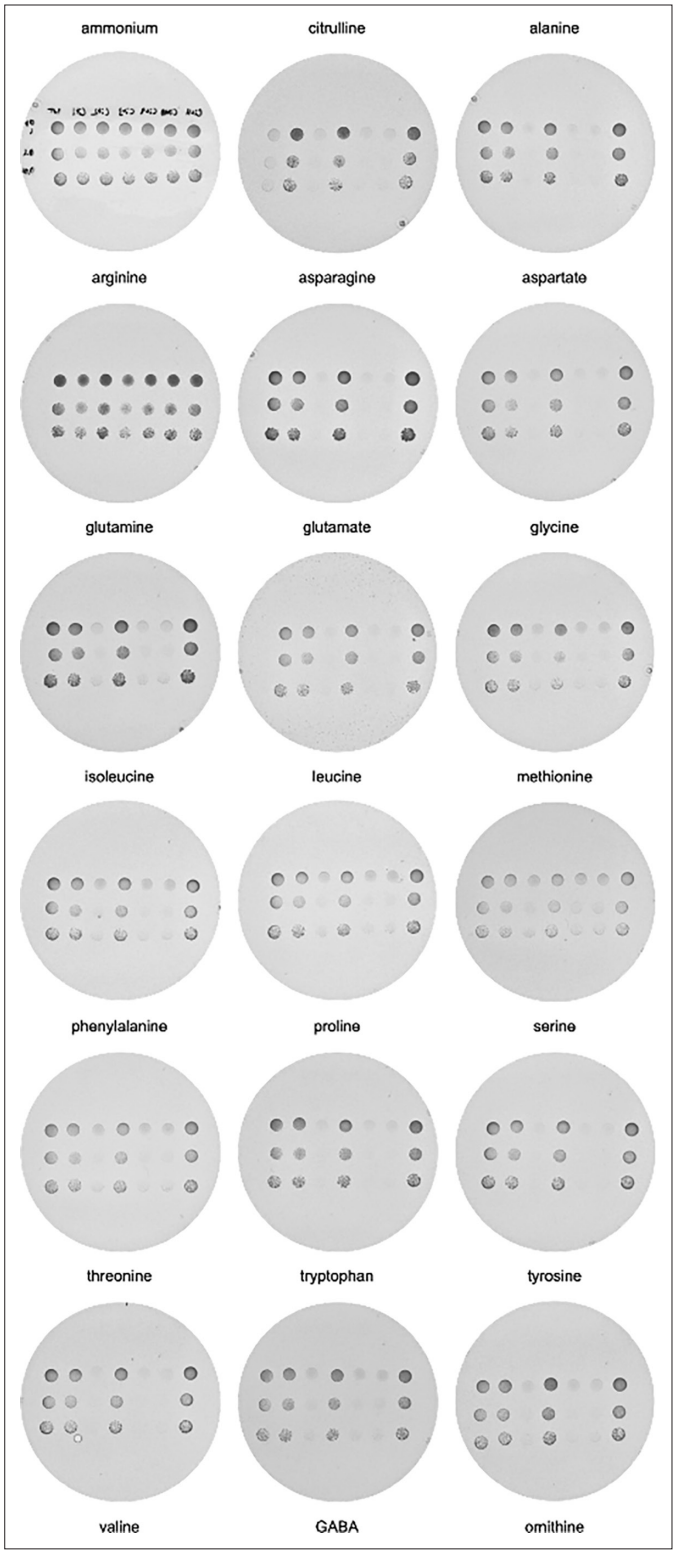

Figure 2—figure supplement 1. In vivo evolution of *AGP1*. Growth assays of Δ10AA pADHXC3GH-*AGP1* variants isolated from Cit evolution, spotted on minimal agar with 1 mM of the respective amino acid as the sole nitrogen source. Dishes were imaged after 6 days of incubation at 30°C. Order of *AGP1* variants in each dish from left to right: *AGP1* wild-type, *AGP1*-Cit1, *AGP1*-Cit2, *AGP1*-Cit3, *AGP1*-Cit9, *AGP1*-Cit10, *AGP1*-Cit11. Spotted are 5 µL of OD_{600} of 1, 0.1, and 0.01.

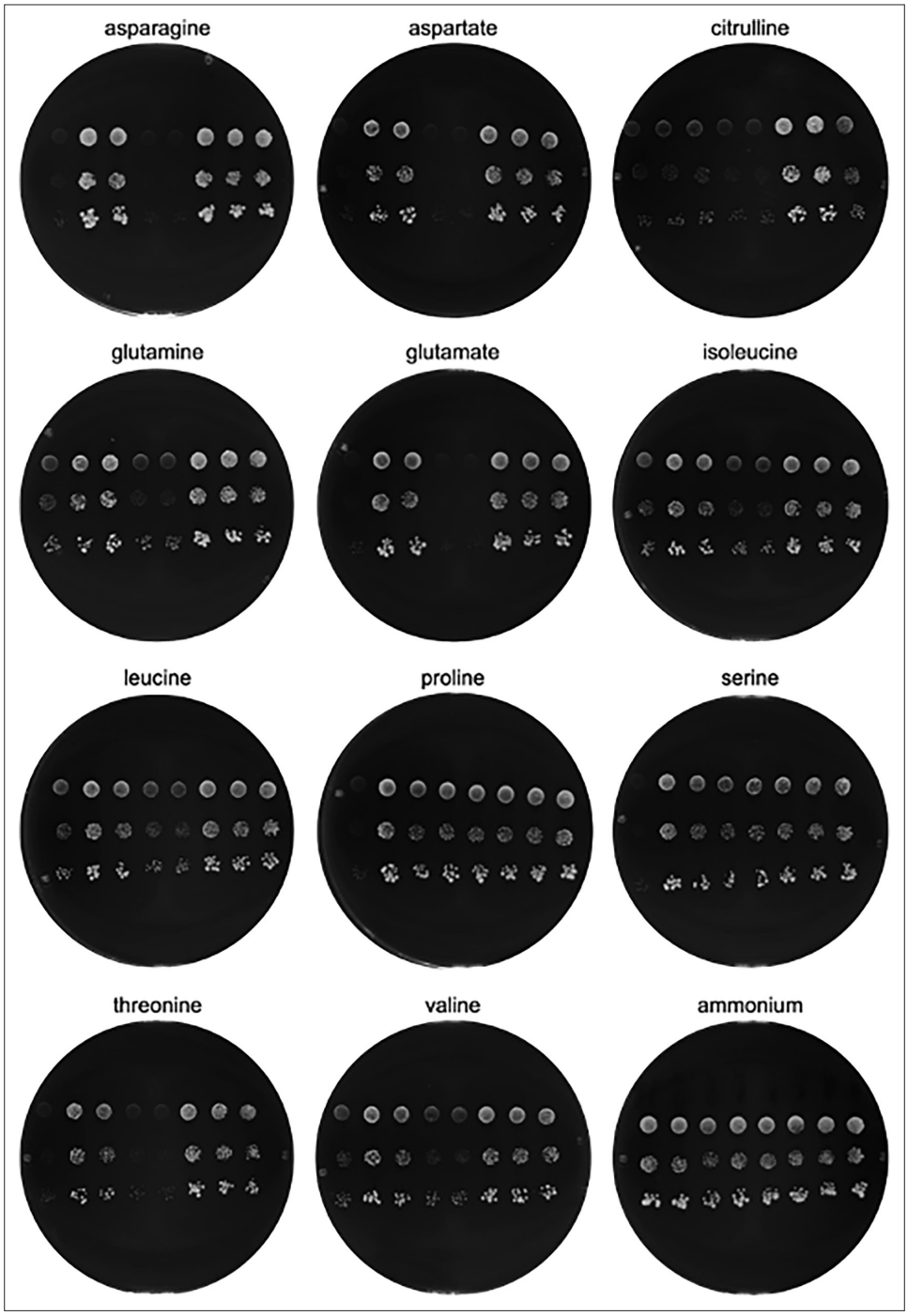

Figure 2—figure supplement 2. In vivo evolution of *PUT4*. Growth assays of Δ10AA pADHXC3GH-*PUT4* variants isolated from Asp and Glu evolution, spotted on minimal agar with 1 mM of the respective amino acid as the sole nitrogen source. Dishes were imaged after 15 days of incubation at 30°C. Order of *PUT4* variants in each dish from left to right: negative control (*AGP1*-Cit9), *PUT4*-Glu2, *PUT4*-Glu1, *PUT4*-wild-type, *PUT4*-wild-type, *PUT4*-Asp3, *PUT4*-Asp2, *PUT4*-Asp1. Spotted are 5 μL of OD_{600} of 0.1, 0.01, and 0.001.

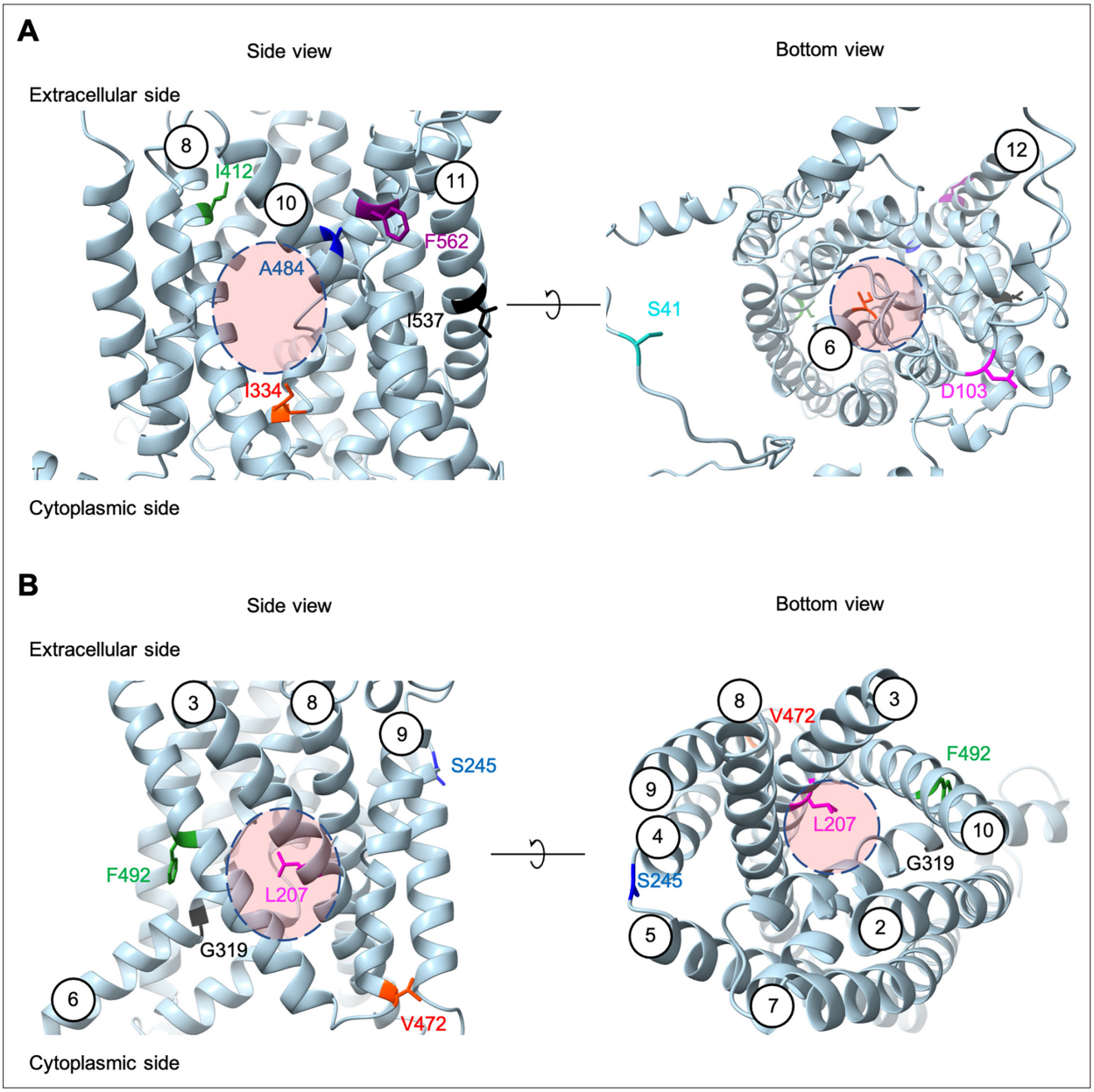

Figure 2—figure supplement 3. Positions of the substituted amino acids found in the evolved mutants. Side and bottom views of the AlphaFold models of *AGP1* (AF-P25376) (**A**) and *PUT4* (AF-P15380) (**B**) visualized in ChimeraX (1.3.0). The reported amino acids that were substituted in the evolved mutants are highlighted in different colors. The respective TMs are presented in circles. The predicted substrate binding site is represented as dashed circle.

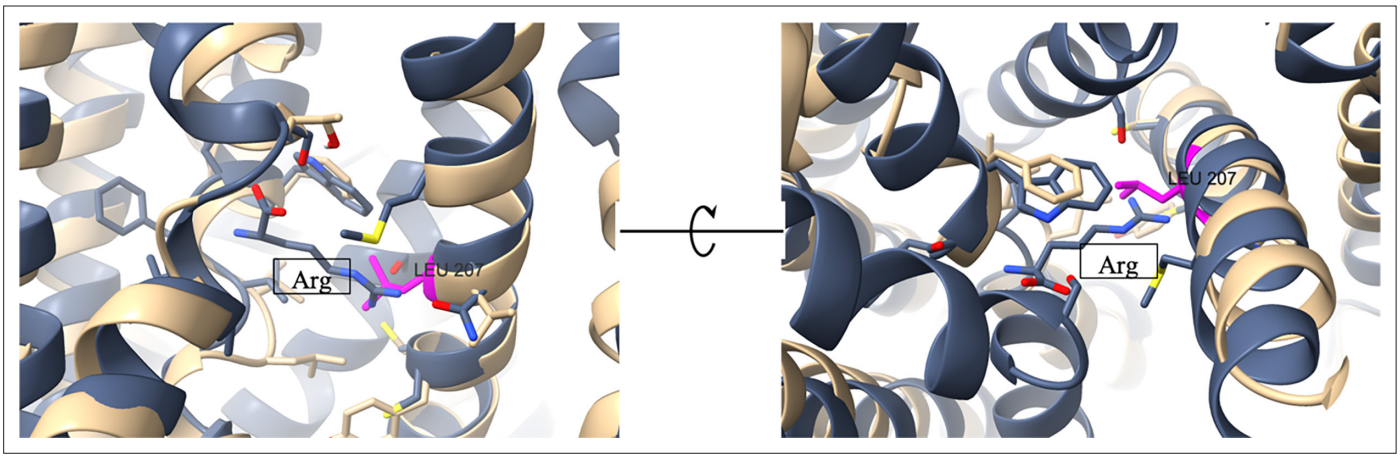

Figure 2—figure supplement 4. Position of the L207S on the transporter's binding site. Overlay of *AdiC* crystal structure (PDB: 3OB6; gray) and *PUT4* AlphaFold model (AF-P15380; beige). The original substrate of *AdiC* is present in the middle of the images ('Arg'; gray). The amino acids contributing to the substrate binding site are shown in sticks. The L207 of *PUT4* is shown in magenta, positioned in the binding site area. According to VAST Search (NCBI), the two structures share a 16.5% sequence identity in the superimposed protein parts, a structural similarity score of 22.15 and RMSD of 3.51 Å.

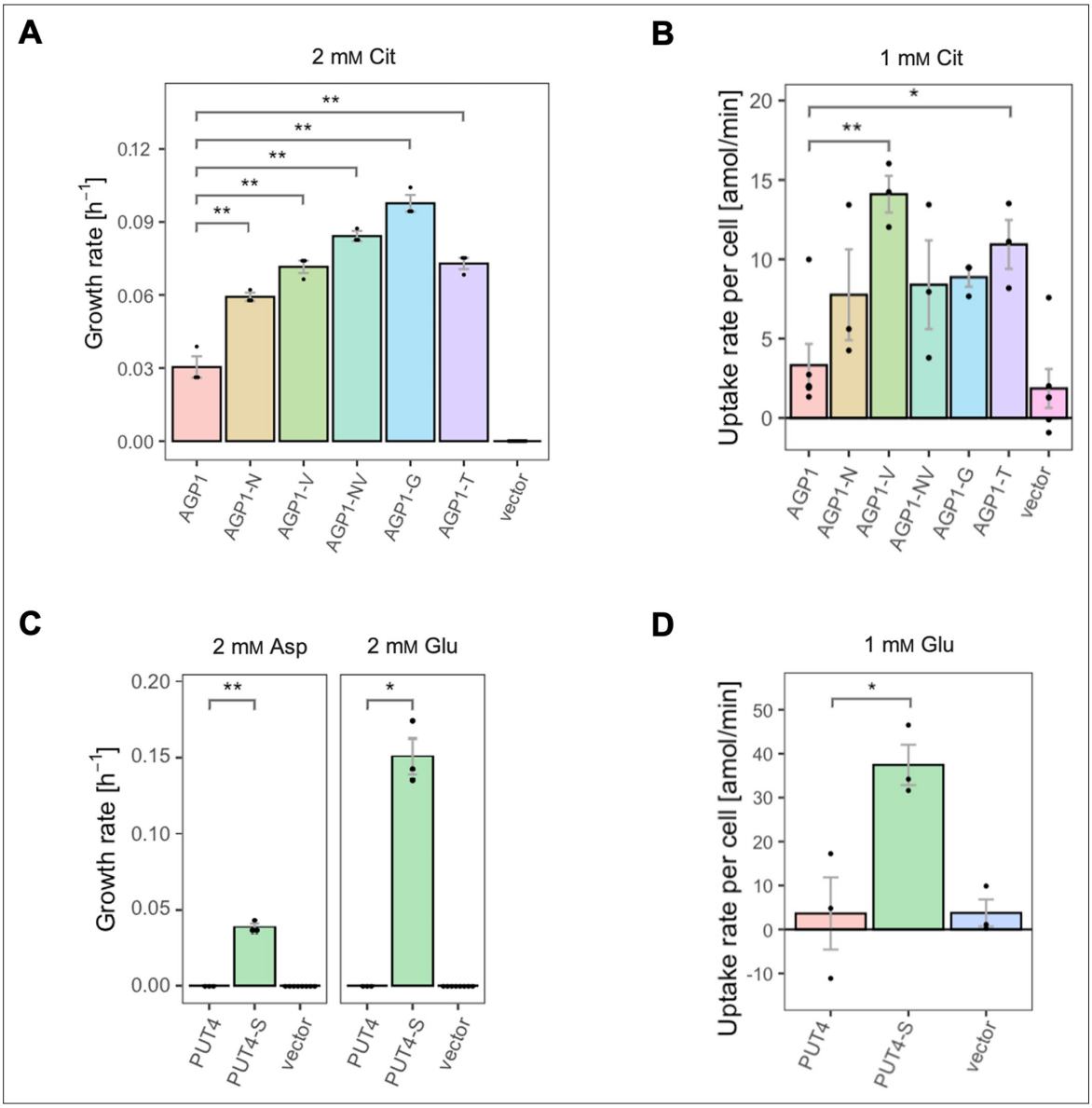

Figure 3. The evolved variants support growth and uptake of the respective amino acids. (**A**) Growth rate of the *AGP1* variants and the vector control on 2 mM L-citrulline (Cit). Error bars represent the SEM (n≥3). (**B**) Uptake rate of 1 mM ^{14}C-Cit by whole cells expressing different *AGP1* variants or none (vector control). Error bars represent the SEM (n≥3). Asterisks in (**A**) and (**B**) indicate the degree of significant difference (one-way ANOVA with a Dunett's test; **p<0.01, *p<0.05) between the *AGP1* variants and wild-type. In case of no significant difference (p>0.05) no asterisks are shown. (**C**) Growth rate of the *PUT4* variants and the vector on 2 mM Asp and Glu. Error bars represent the SEM (n≥3). (**D**) Uptake rate of 1 mM ^{14}C-Glu by whole cells expressing different *PUT4* variants or none (vector control). Error bars represent the SEM (n≥3). Asterisks in (**C**) and (**D**) indicate the degree of significant difference in pairwise comparisons between the transporter-expressing variants (Student's t-test; **p<0.01, *p<0.05).

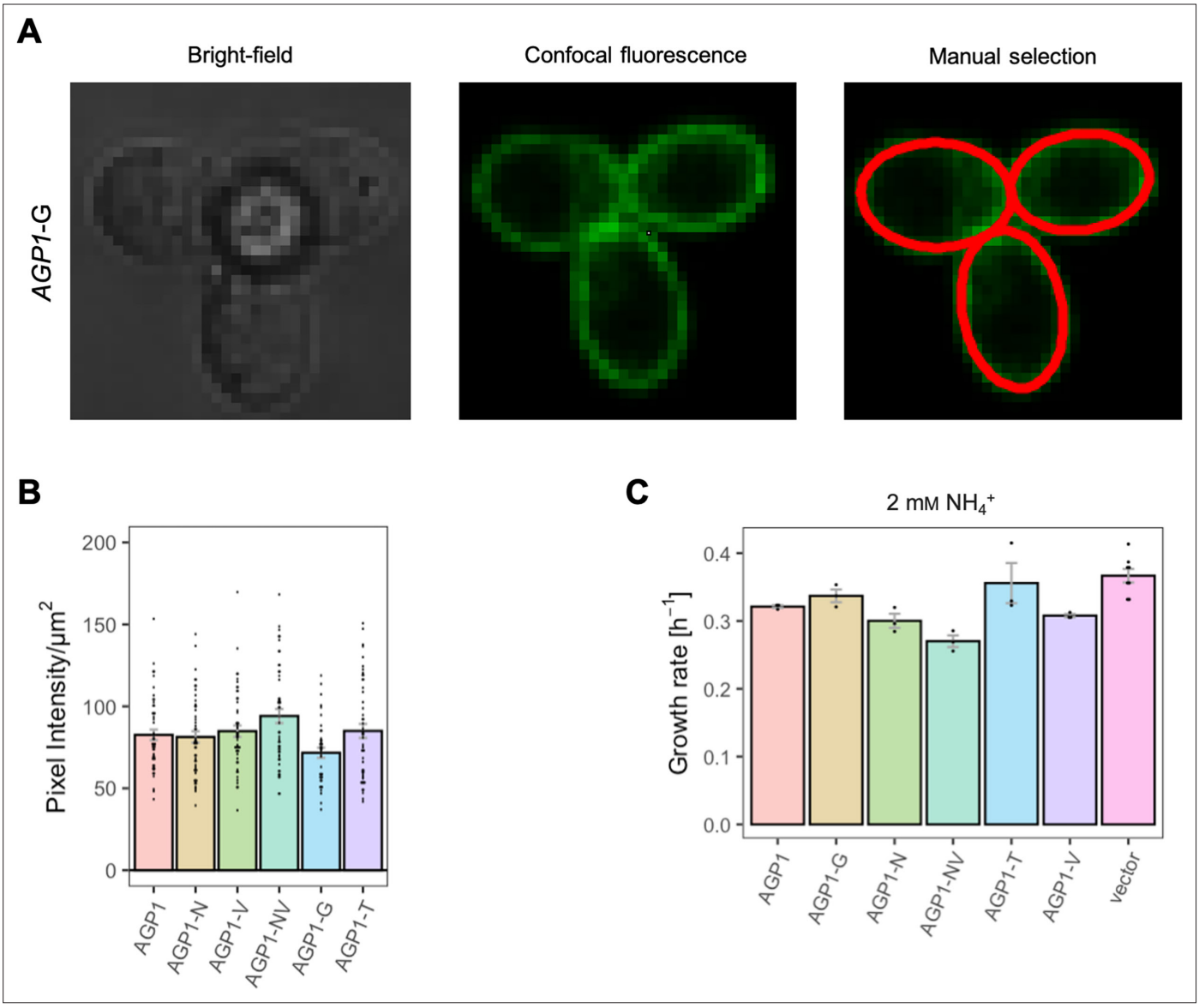

Figure 3—figure supplement 1. Effects of evolved *AGP1* mutations on the surface expression and growth on non-amino acid nitrogen source. (**A**) Localization of the *AGP1*-G variant in whole cells by fluorescence microscopy. The same cells are presented under the bright-field (left) and confocal fluorescence (middle) channels. The manual selection of the periphery of the cells (right) was performed in Fiji with 1 pixel width. (**B**) Surface expression of the *AGP1* variants. Error bars represent the SEM (n=40–50). (**C**) Growth rate of the *AGP1* variants and the vector on 2 mM NH_4^+. Error bars represent the SEM (n≥3). One-way ANOVA with a Dunett's test showed no significant difference between the *AGP1* variants and wild-type for both (**B**) and (**C**).

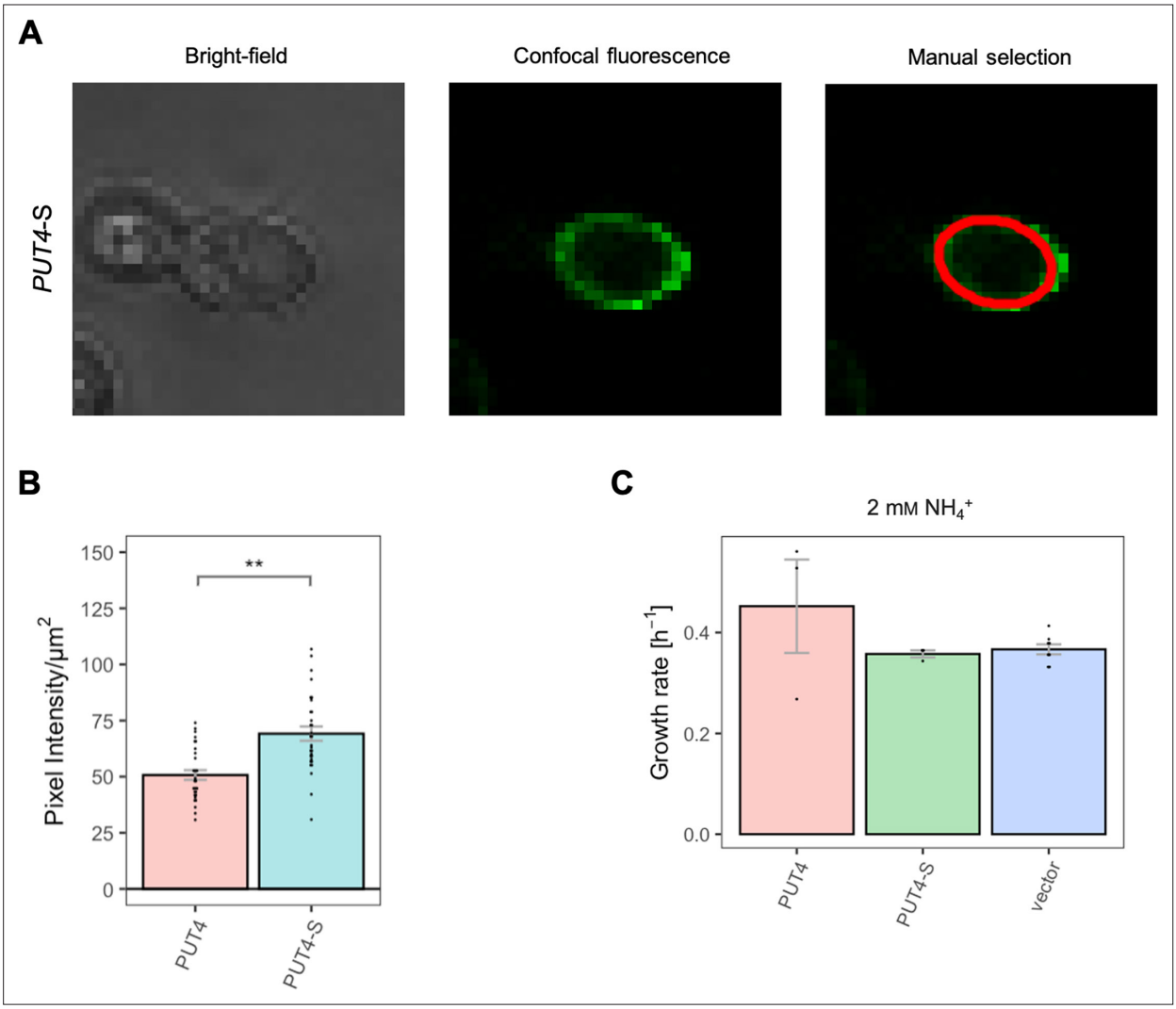

Figure 3—figure supplement 2. Effects of evolved *PUT4*-S mutation on the surface expression and growth on non-amino acid nitrogen source. (**A**) Localization of the *PUT4*-S variant in whole cells by fluorescence microscopy. The same cell is presented under the bright-field (left) and confocal fluorescence (middle) channels. The manual selection of the periphery of the cell (right) was performed in Fiji with 1 pixel width. (**B**) Surface expression of the *PUT4* variants. Error bars represent the SEM (n=30). Asterisks indicate the degree of significant difference in pairwise comparison between the transporter-expressing variants (Student's t-test; **p<0.01, *p<0.05). (**C**) Growth rate of the *PUT4* variants and the vector on 2 mM NH_4^+. Error bars represent the SEM (n≥3). Pairwise comparison (Student's t-test) showed no significant difference between the transporter-expressing variants.

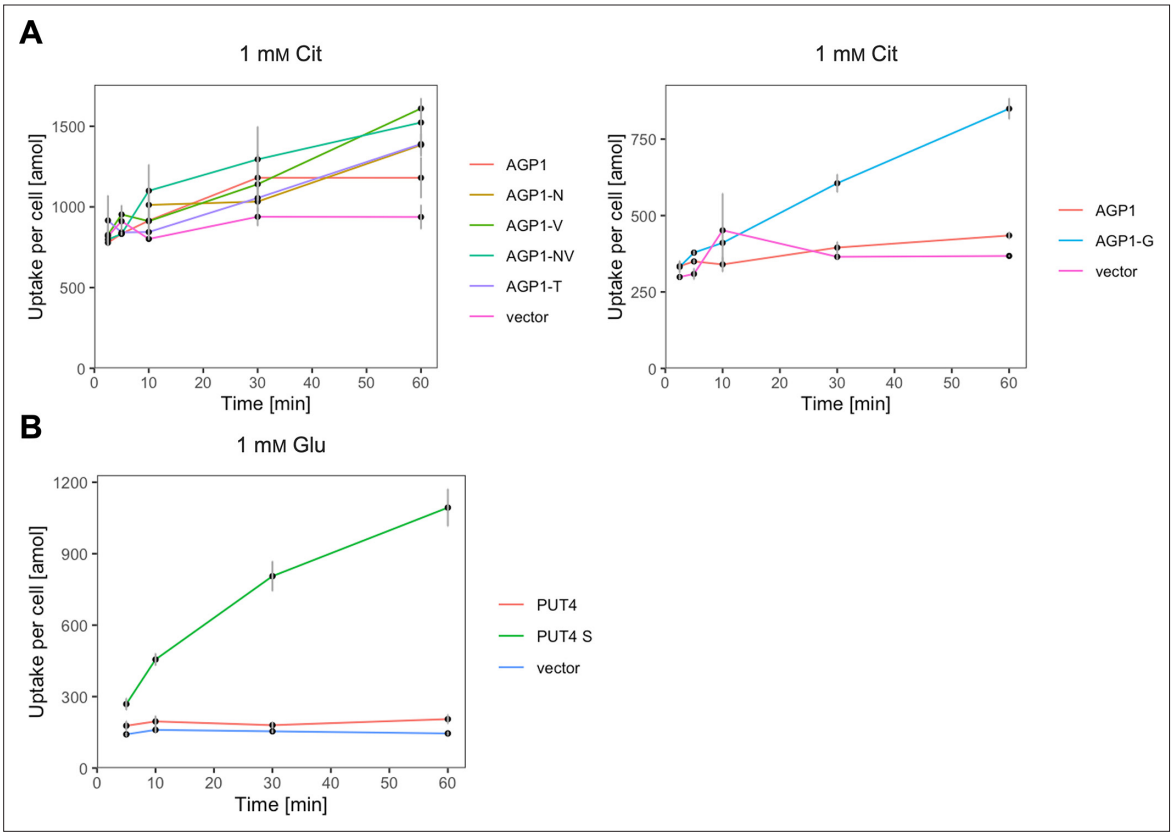

Figure 3—figure supplement 3. The evolved variants support uptake of the respective amino acids. (**A**) Uptake of 1 mM ^{14}C-Cit by whole cells expressing different *AGP1* variants or none (vector). Error bars represent the SD (n=3). Each graph represents an independent experiment. (**B**) Uptake of 1 mM ^{14}C-Glu by whole cells expressing different *PUT4* variants or none (vector). Error bars represent the SD (n=3).

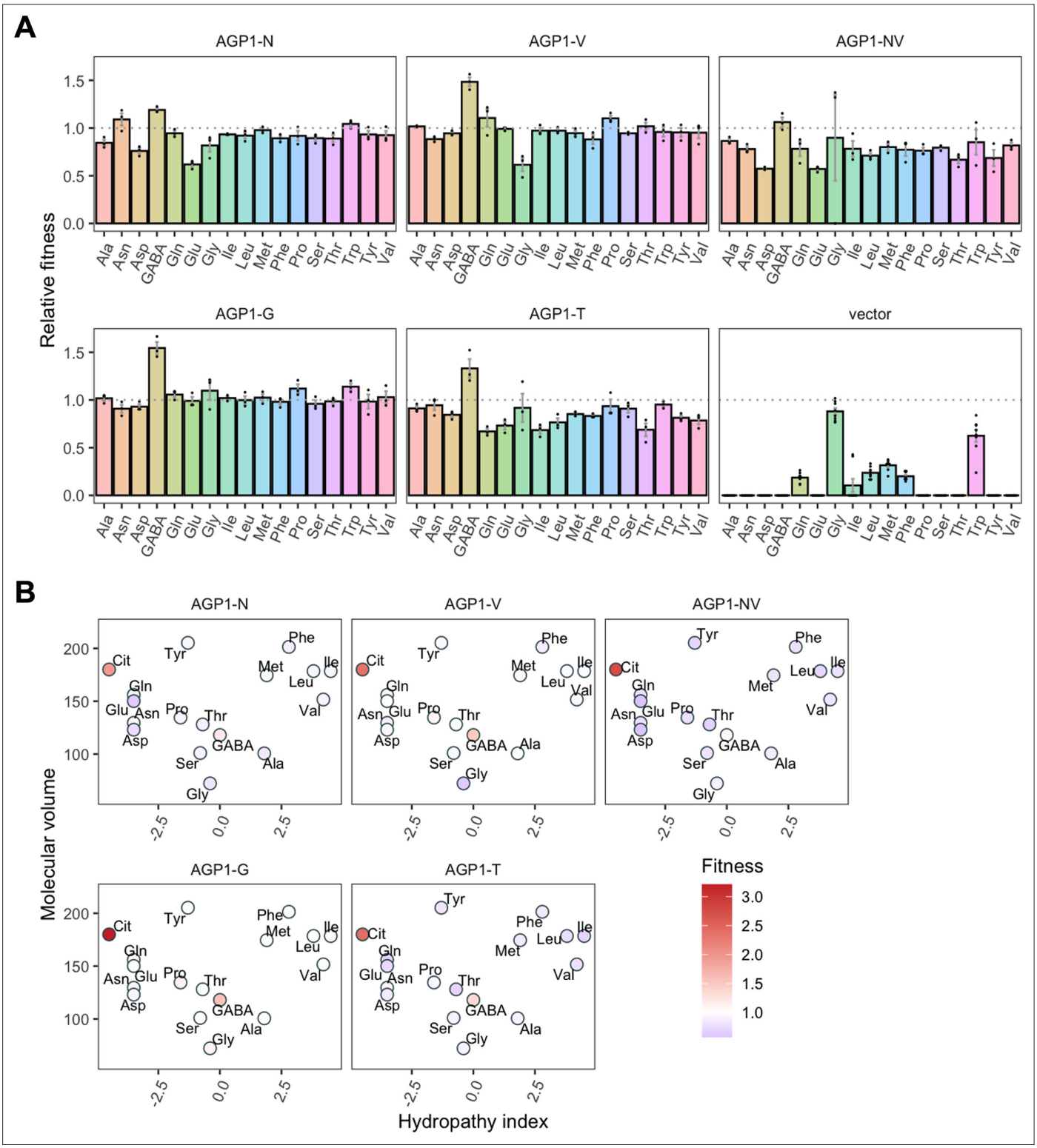

Figure 4. Relative fitness of evolved *AGP1* variants. (**A**) Relative fitness of *AGP1* variants and the control strain for the growth on each of 17 amino acids as the sole nitrogen source. The relative fitness was calculated separately for each amino acid by dividing the growth rate of the mutant by the mean growth rate of the wild-type *AGP1*. Error bars represent the SEM (n≥3). For the respective growth curves, see ***Figure 4—figure supplement 1***. (**B**) Mean relative fitness of *AGP1* variants per substrate as a function of the amino acid hydropathy index (x axis) and molecular volume (y axis). Color corresponds to relative fitness. The plot is based on the growth rate measurements of panel (**A**).

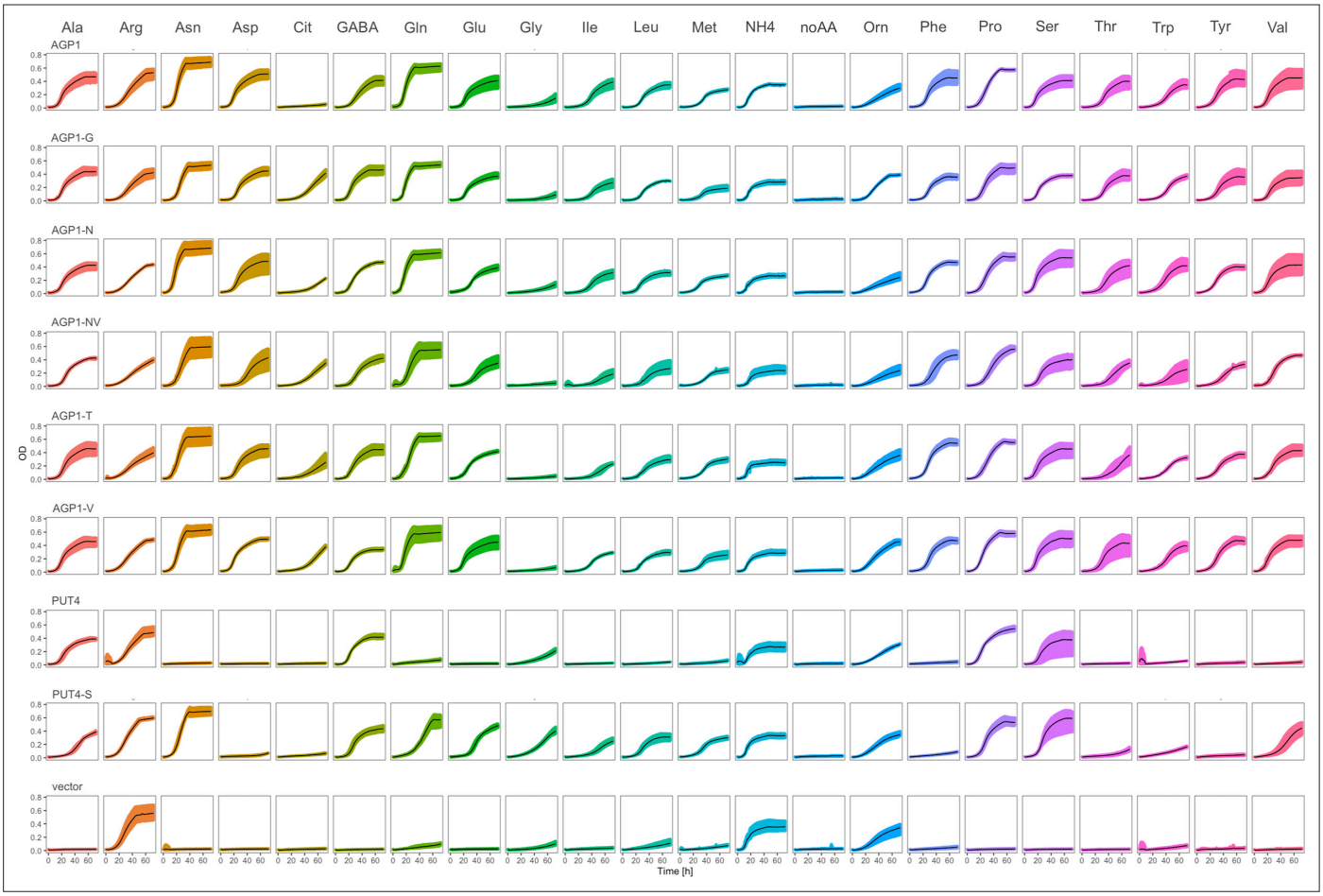

Figure 4—figure supplement 1. The evolved variants affect the strain's growth on different amino acids. Growth curves of Δ10AA expressing either one of the *AGP1* and *PUT4* variants from pADHXC3GH and the empty vector control on 2 mM of each amino acid. Black lines represent mean values of all measured curves (n≥3). Colored areas represent the SD range.

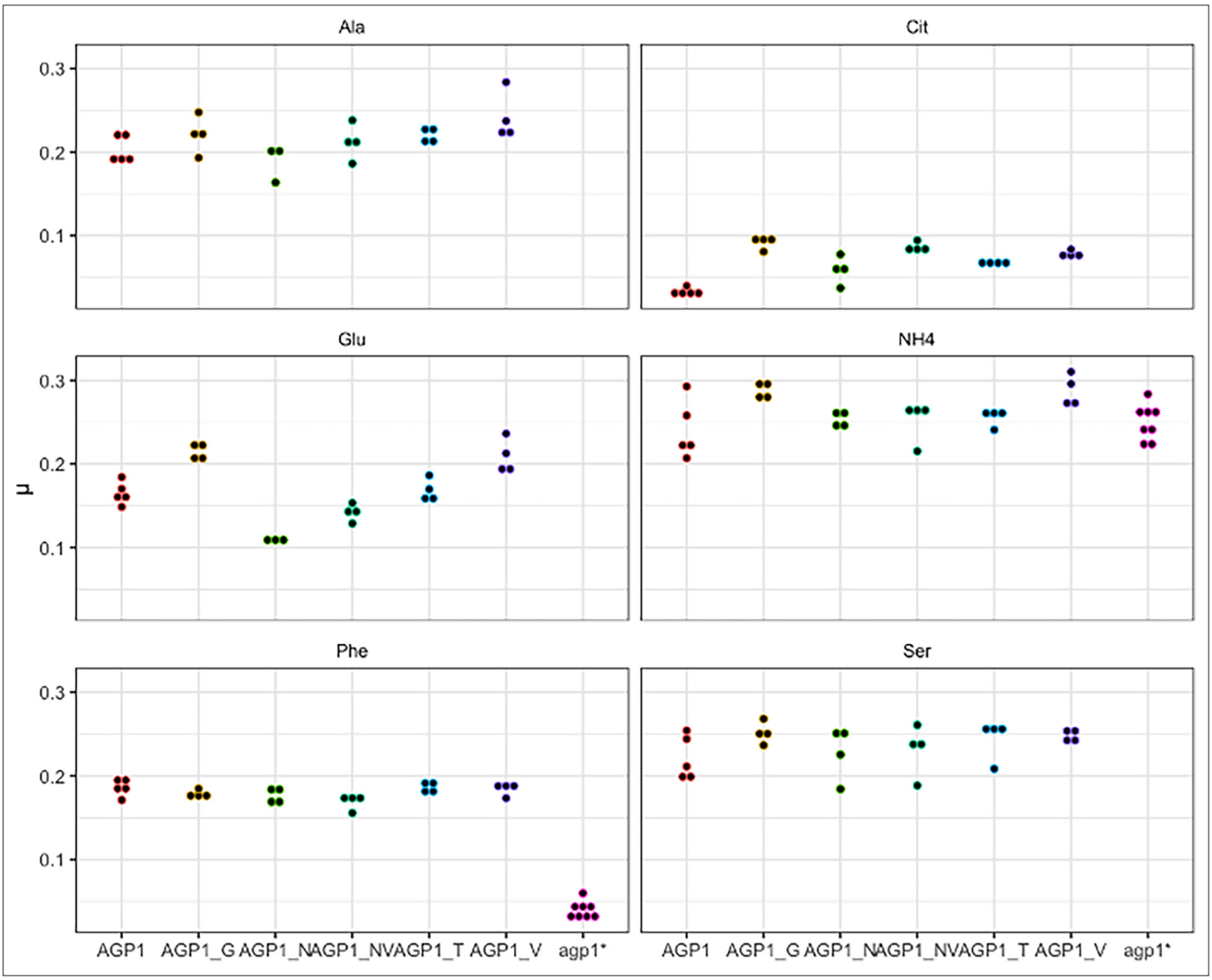

Figure 4—figure supplement 2. Effects of evolved *AGP1* mutations on the growth rate on original substrates. Repetition of the growth rate (μ) measurements of Δ10AA expressing either one of the *AGP1* variants from pADHXC3GH on selected substrates. Each point reflects the growth rate of one replicate culture. Note the slow growth of wild-type *AGP1* on Cit.

Figure 5. Effects of evolved *AGP1* mutations on the growth and uptake of original substrates. (**A**) Localization of the *AGP1* variants in whole cells, based on replicate samples (different colonies) and analyzed by fluorescence microscopy, including a zoom-in of a representative cell. (**B**) Growth rate of the *AGP1* variants and the vector on 2 mM Glu. Error bars represent the SEM (n≥3). (**C–D**) Uptake rate of 0.1 (**C**) and 2 mM (**D**) ^{14}C-Glu in whole cells expressing different *AGP1* variants or none (vector control). In the case of *AGP1*-G, the assay was performed with 2 mM ^{3}H-Glu and is presented as independent experiment. Error bars represent the SEM (n≥3). (**E**) Growth rate of the *AGP1* variants and the vector control on 2 mM Phe. Error bars represent the SEM (n≥3). (**F–G**) Uptake rate of 0.1 (**F**) and 2 mM (**G**) ^{14}C-Phe in whole cells expressing different *AGP1* variants or none (vector control).

Figure 5 continued on next page

Figure 5 continued

Error bars represent the SEM (n≥3). Asterisks in (**B–G**) indicate the degree of significant difference (one-way ANOVA with a Dunett's test; **p<0.01, *p<0.05) between the *AGP1* variants and wild-type. In case of no significant difference (p>0.05), no asterisks are shown. For the respective uptake curves, see ***Figure 5—figure supplement 1***.

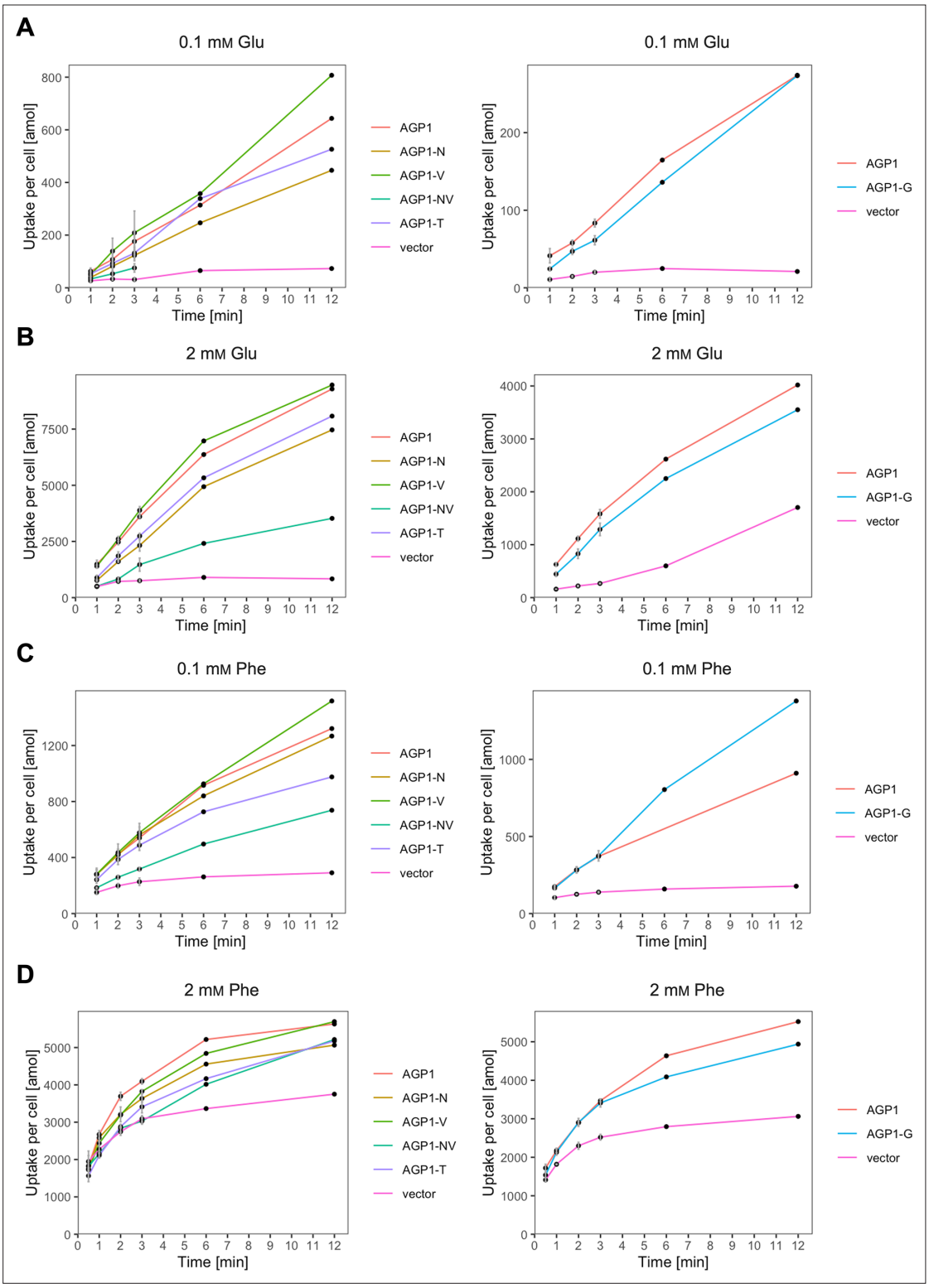

Figure 5—figure supplement 1. The evolved *AGP1* variants support uptake of original substrates. Uptake of 0.1 mM ^{14}C-Glu (**A**), 2 mM ^{14}C-Glu (B; left), or ^{3}H-Glu (B; right), 0.1 mM ^{14}C-Phe (**C**), 2 mM ^{14}C-Phe (**D**) by whole cells expressing different *AGP1* variants or none (vector). Error bars represent the SD (n=3). Each graph represents an independent experiment from the uptakes described in ***Figure 5***.

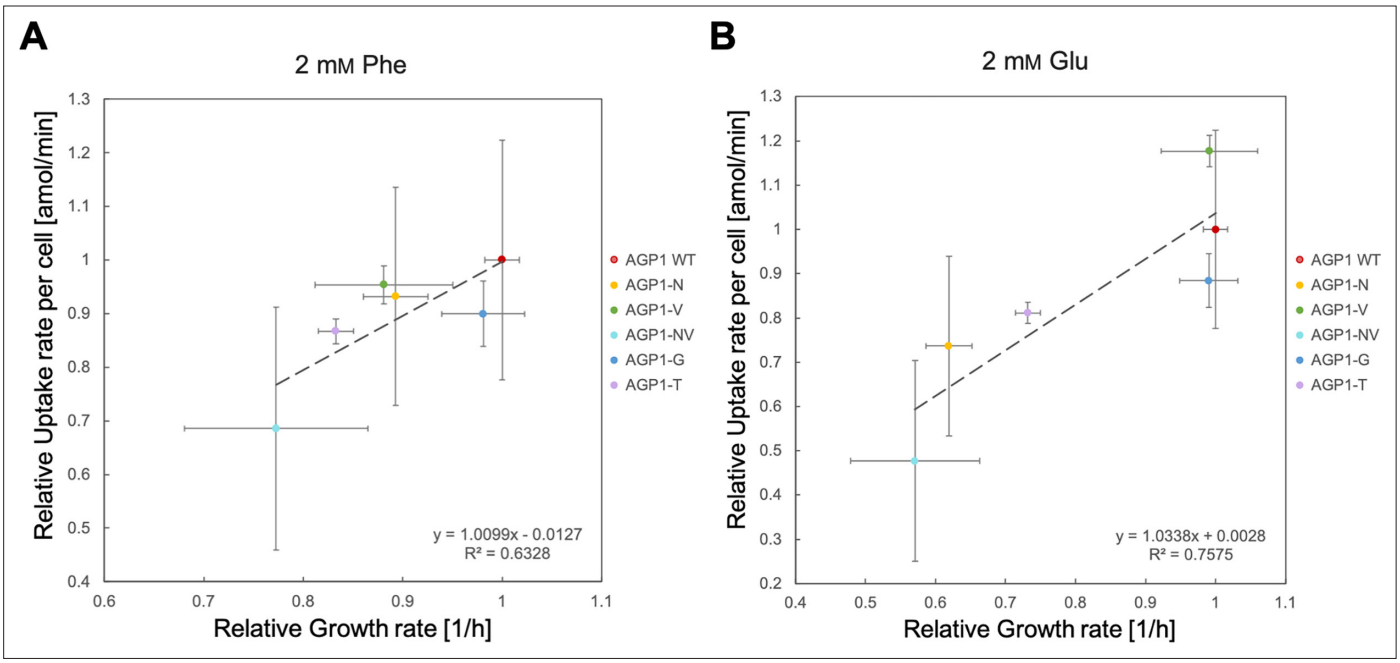

Figure 5—figure supplement 2. Correlation between the fitness and uptake of original substrates for the evolved *AGP1* variants. The uptake rate and growth rate on 2 mM Phe (**A**) or Glu (**B**) for the evolved *AGP1* variants is presented relative to that of cells expressing the wild-type protein. Error bars represent the SD (n≥3). The correlation is described by the linear regression trendline and the equation is shown in the graph.

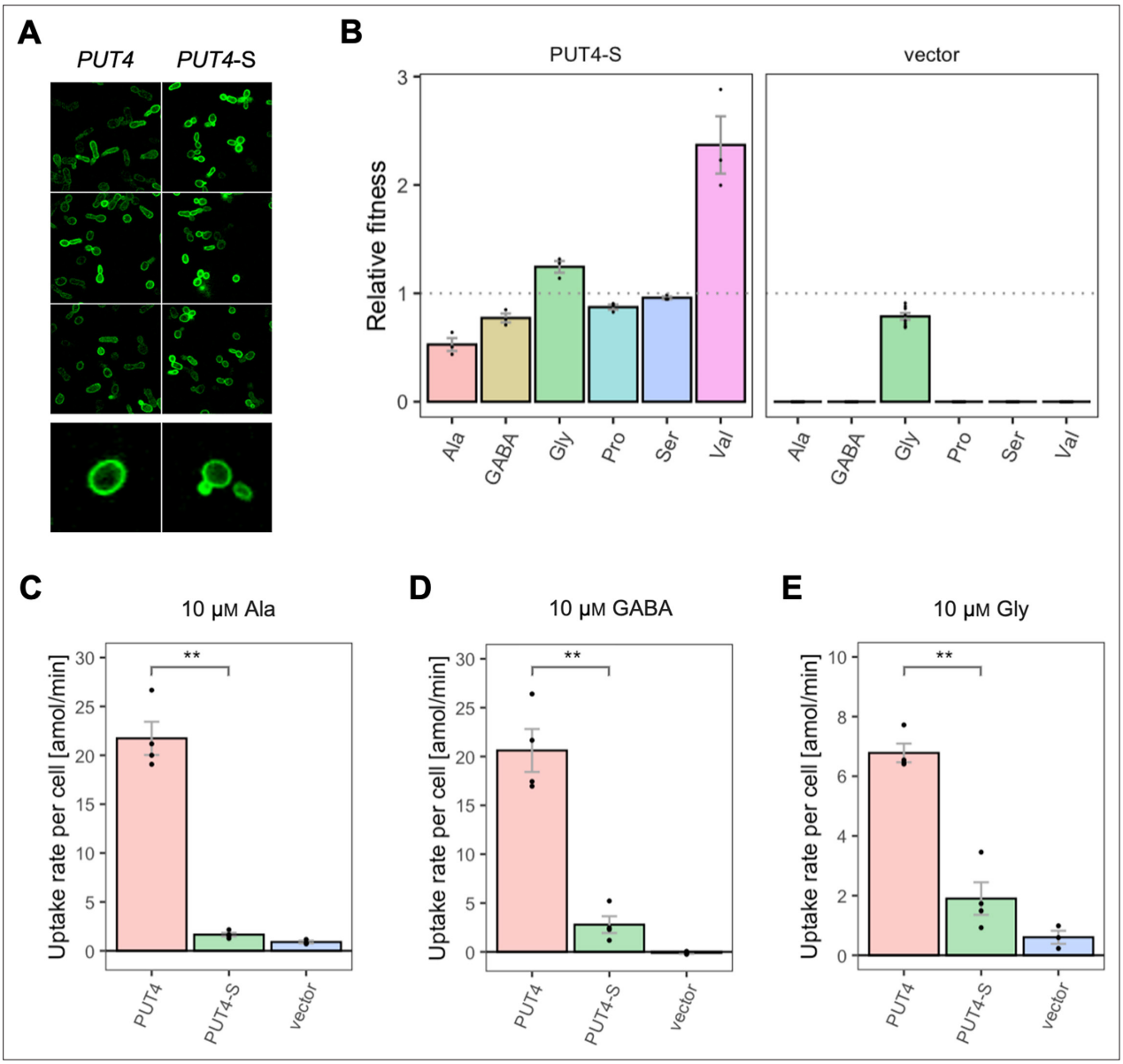

Figure 6. Effects of evolved *PUT4*-S mutation on the growth and uptake of original substrates. (**A**) Localization of the *PUT4* variants in whole cells, based on replicate samples (different colonies) and analyzed by fluorescence microscopy, including a zoom-in of a representative cell. (**B**) Relative fitness of *PUT4*-S and the vector for the growth on six amino acids as the sole nitrogen source. The relative fitness was calculated separately for each amino acid by dividing the growth rate of the mutant by the mean growth rate of the wild-type *PUT4*. Error bars represent the SEM (n≥3). For the respective growth curves, see ***Figure 4—figure supplement 1***. (**C–E**) Uptake rate of 10 μM ^{14}C-Ala (**C**), γ-amino butyric acid (GABA) (**D**), or Gly (**E**) in whole cells expressing *PUT4* variants or none (vector). Error bars represent the SEM (n≥3). Asterisks in (**C–E**) indicate the degree of significant difference in pairwise comparisons between the transporter-expressing variants (Student's t-test; **p<0.01, *p<0.05). For the respective uptake curves, see ***Figure 6—figure supplement 1***.

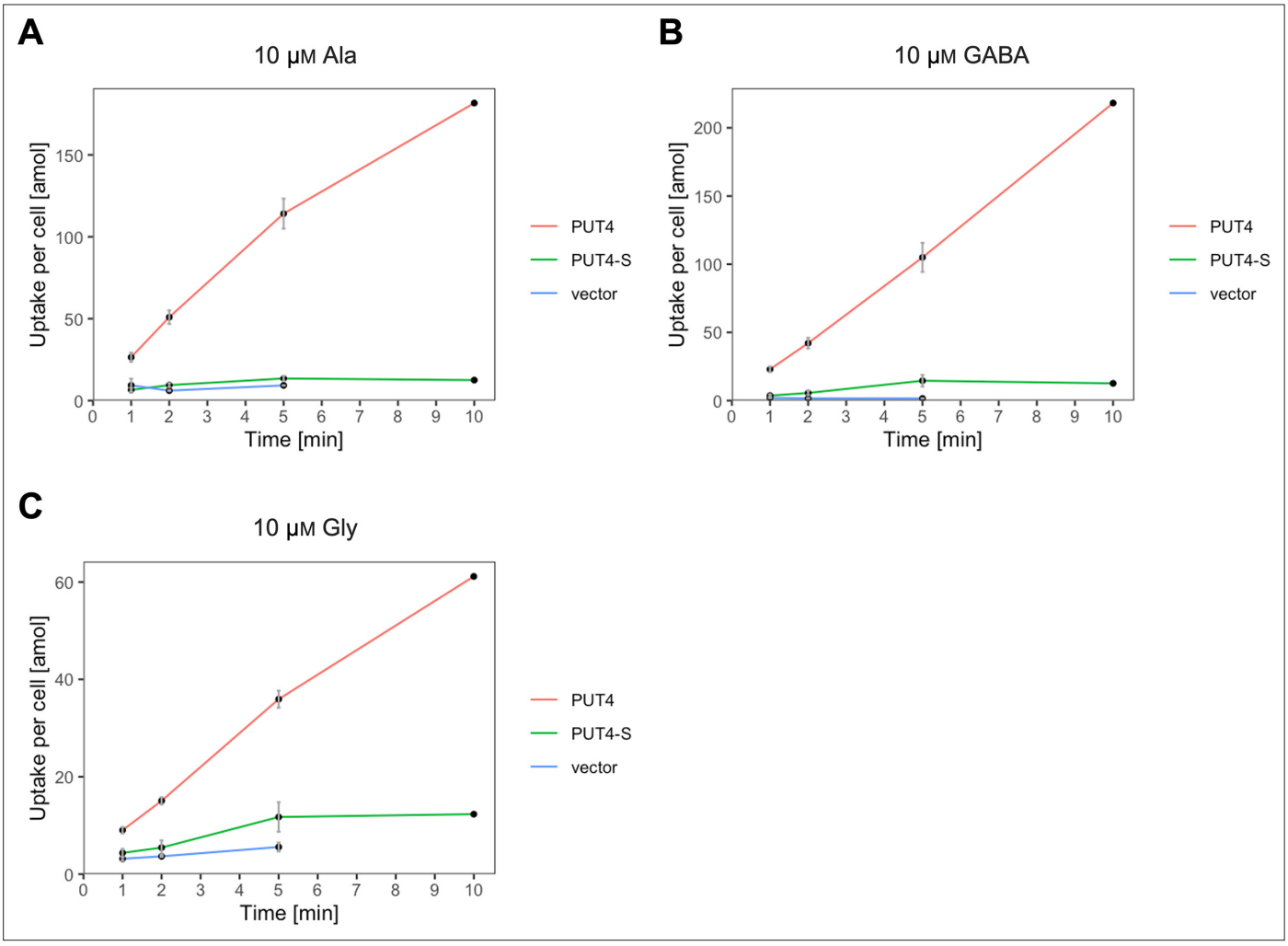

Figure 6—figure supplement 1. The evolved *PUT4* variant supports uptake of original substrates. Uptake of 10 μM ^{14}C-Ala (**A**), γ-amino butyric acid (GABA) (**B**), or Gly (**C**) by whole cells expressing different *PUT4* variants or none (vector). Error bars represent the SD (n=3). Each graph represents an independent experiment from the uptakes described in ***Figure 6***.

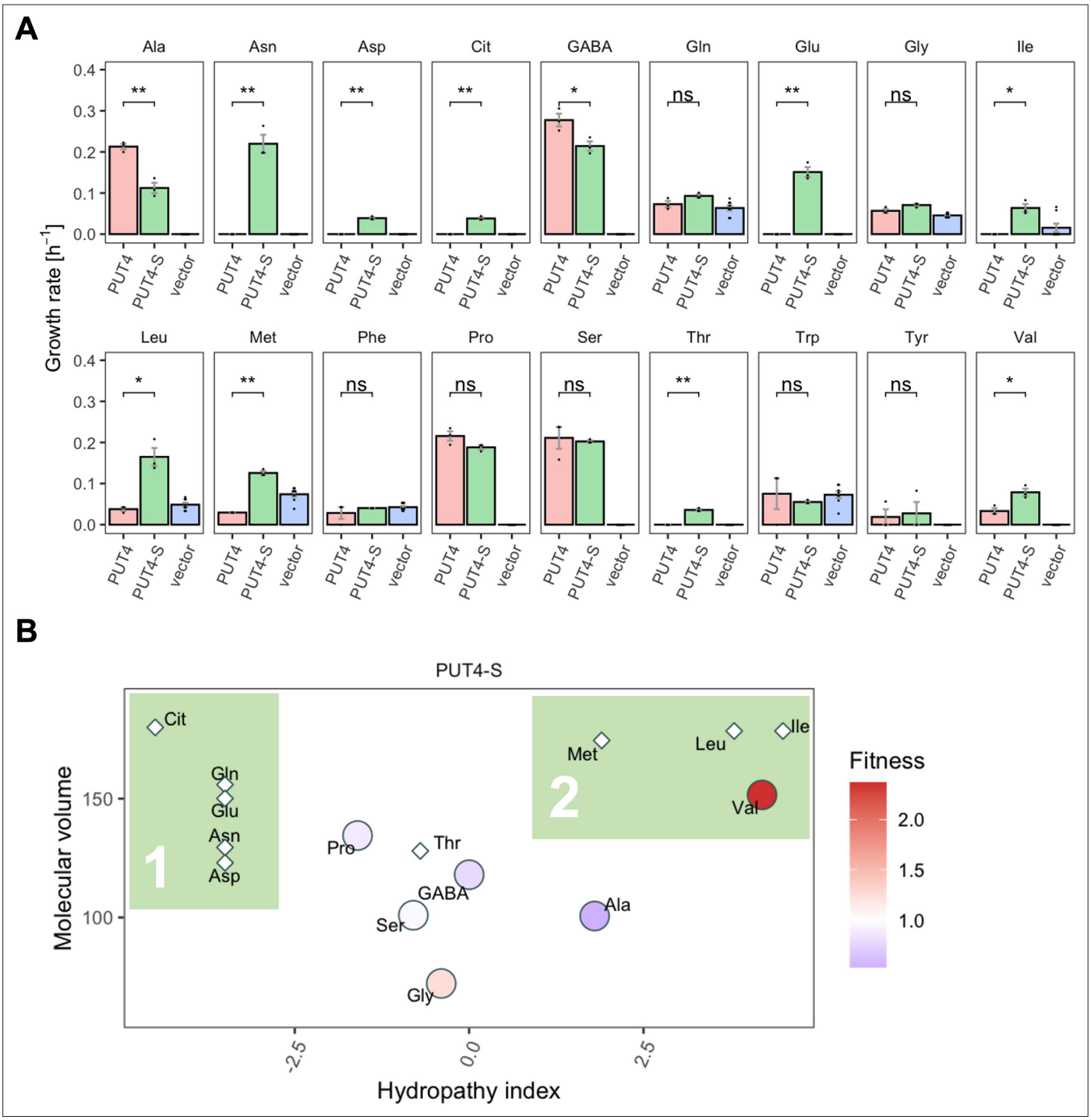

Figure 7. The evolved *PUT4*-S mutation broadens the substrate range of the transporter. (**A**) Growth rate measurements of *PUT4* variants and the vector control on 2 mM of 18 different amino acids as the sole nitrogen source. Error bars represent the SEM (n≥3). Asterisks indicate the degree of significant difference in pairwise comparisons (Student's t-test; **p<0.01, *p<0.05). For the respective growth curves, see ***Figure 4—figure supplement 1***. (**B**) Mean relative fitness of *PUT4*-S per substrate as a function of the amino acid hydropathy index (x axis) and molecular volume (y axis). Diamond shapes indicate novel substrates not found in the wild-type *PUT4*. Color corresponds to relative fitness. The plot is based on the same growth rate measurements as (**A**).